JOURNAL OF CATALYSIS **133**, 461–466 (1992)

A Reason for the Structure-Insensitive Catalytic Activity of Ni(100) and Ni(111) Surfaces for the Methanation Reaction of CO

HIDEKI HIRANO AND KEN-ICHI TANAKA[1]

Institute for Solid State Physics, University of Tokyo, 7-22-1 Roppongi, Minato-ku, Tokyo 106, Japan

Received January 16, 1991; revised August 21, 1991

The structure-insensitive methanation reaction, $CO + 3H_2 \rightarrow CH_4 + H_2O$, on Ni(111) and Ni(100) surfaces (*1, 2*), is rationalized on the basis of the structure of carbidic carbon intermediates. Accumulation of carbidic carbon intermediates on the Ni(100) surface results in a (2 × 2)p4g overlayer, and its hydrogenation proceeds at a rate almost equal to that of a steady-state methanation reaction. In contrast to the carbide overlayer on the Ni(100) surface, the LEED pattern of the carbide overlayer on the Ni(111) surface is too complex to be solved. A single-domain carbide on a Ni(111) surface accidentally obtained by the segregation of carbon allowed us to deduce the structure of the carbide overlayer on the Ni(111) surface. It was shown that the carbide overlayer on Ni(111) has exactly the same arrangement of carbon atoms as that of the (2 × 2)p4g structure on the Ni(100) surface. In addition, the carbide overlayer undergoes decomposition at 685 K on Ni(100), Ni(110), and Ni(111) surfaces. Therefore, we conclude that the accumulation of carbidic intermediates creates an identical surface carbide on Ni(100) and Ni(111) surfaces. This may be a reason for the structure-insensitive catalysis, because the methanation may be catalyzed by this surface carbide on Ni(100) and Ni(111) surfaces.

INTRODUCTION

Goodman *et al.* (*1, 2*) demonstrated that carbidic carbon is a key intermediate in the methanation reaction, and the amount of carbide during catalysis is controlled by a dynamic balance between the deposition and the hydrogenation of carbidic carbon intermediates. Furthermore, Goodman *et al.* showed that the turnover number for methane formation, $CO + 3H_2 \rightarrow CH_4 + H_2O$, is almost the same on Ni(100) and Ni(111) surfaces.

On the other hand, it is well known that the carbide overlayer on Ni(100) and that on Ni(111) give quite different LEED patterns as shown in Figs. 1a and 1b; Fig. 1a is a pattern of the (2 × 2)P4g structure (*5*). If the carbide overlayer on Ni(100) and Ni(111) surfaces corresponds to the intermediates in the methanation reaction, a question may arise why the methanation reaction proceeds at nearly the same rate as on Ni(100) and Ni(111) surfaces? So far, no persuasive explanation has been given for such a structure-independent activity of the methanation reaction on Ni(100) and Ni(111) surfaces. To shed light on this interesting feature in catalysis, the molecular mechanism based on the structure of the intermediates must be known.

The mechanism of formation of carbidic carbon intermediates is still obscure, but two probable mechanisms, unimolecular dissociation of the CO molecule (*7*) and the dismutation reaction of CO (*3, 4*), have been proposed. The amount of carbided carbon on the surface during the reaction depends on a balance between the formation and the consumption of the carbidic carbon intermediates. Therefore, accumulation of carbidic carbon intermediates is expected when the hydrogen pressure becomes low and the dismutation reaction of CO, $2CO \rightarrow C + CO_2$, reflects a limited case of $H_2 = 0$. We can prepare one monolayer of carbide on Ni sur-

---

[1] To whom correspondence should be addressed.

0021-9517/92 $3.00

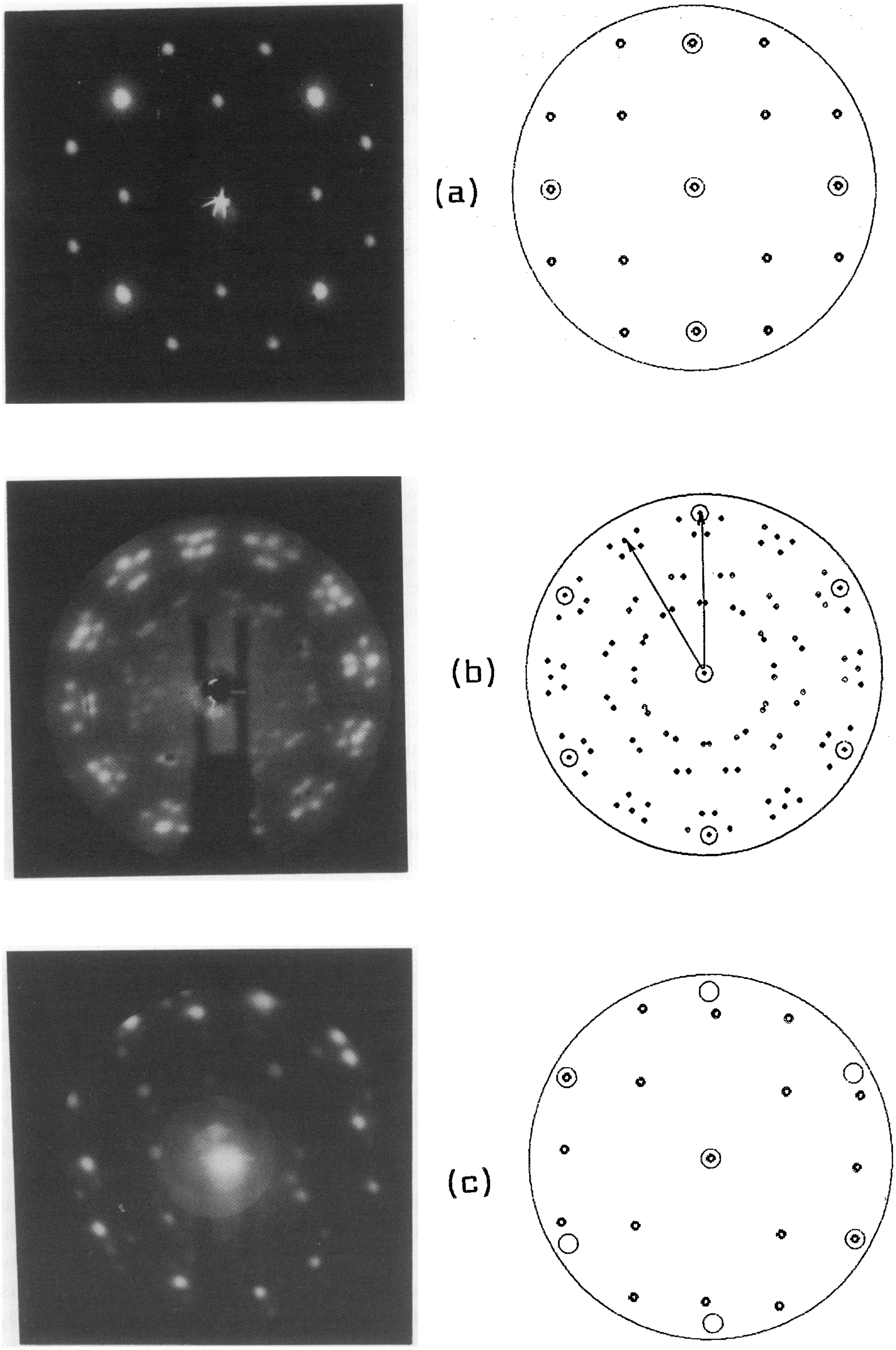
(a)
(b)
(c)

faces by segregation of impurity carbon involved in the bulk. Therefore, these two methods were adopted to make one monolayer of carbide on Ni(100), Ni(111), and Ni(110) surfaces.

EXPERIMENTAL

Experiments were performed in UHV chamber equipped with a LEED, a double-focused CMA auger electron spectrometer (AES), a quadrupole mass spectrometer, and a high-pressure reactor of small volume (about 300 ml). By using a long-drive transfer rod, a single-crystal sample was pushed into the high-pressure reactor; the contact between the mirror-polished brim of the sample holder head and a Teflon gasket at the gate of the reactor made a perfect seal between the UHV system and the high-pressure reactor. The details have been described elsewhere (*6*). A single-crystal disk (8 mm in diameter and 1 mm thick) was lifted by spot-welding with two 0.25-mm-diameter Ta wires and was heated by ohmic heating of the Ta wires. The temperature was controlled by a feedback current control system connected to a chromel–alumel thermocouple spot-welded on the edge of the crystal. The Ni(100) and Ni(111) surfaces were cleaned by repeating the cycle of oxidation in O_2 of 10^{-7} Torr at 900 K, Ar ion bombardment at room temperature, and annealing at 1000 K in a vacuum of 10^{-10} Torr. Carbidic carbon was deposited on a clean Ni(100) or Ni(111) surface by performing the dismutation reaction of CO in the high-pressure reactor at desired pressure and temperature for a given time. After the reaction, the ambient gas was quickly evacuated by a turbomolecular pump, and the sample was then pulled back into the UHV chamber for the LEED and AES measurements. The amount of carbon deposited on the Ni surface was evaluated by the AES peak intensity ratio of the C_{KVV} peak at 272 eV to the Ni_{LMM} peak at 848 eV.

RESULTS AND DISCUSSION

Catalytic reactions taking place on solid surfaces have been explained by a concept based on the reaction of adsorbed molecules. As a result, intermediates that are formed on the surface during catalysis have very poor structural identity in heterogeneous catalysis. To understand the mechanism of catalysis, however, structural knowledge of the key intermediates is essential. To deduce the structure of intermediates, the intermediates should be accumulated over the catalyst surface, which is analogous to the isolation of the intermediate complexes in homogeneous catalysis for X-ray diffraction. It should be noted that the isolated intermediates are different from the working catalyst. Therefore, it should be confirmed that the isolated compound acts as an intermediate in the corresponding reaction. Our strategy is to accumulate carbidic carbon intermediates on Ni(100) and Ni(111) surfaces and then subject them to structural analysis as well as to the hydrogenation reaction.

Both the dismutation reaction of CO, $2CO \rightarrow C(a) + CO_2$, and the methanation reaction of CO, $CO + 3H_2 \rightarrow CH_4 + H_2O$, proceed readily at a certain CO pressures but scarcely occur at low CO pressures (*2, 3, 8–10*). In fact, no methane is detected on Ru(110) or on Ni(100) surfaces when the pressure of a mixture of H_2 and CO is lower than 10^{-3} Torr (*11, 12*). In contrast, Astaldi *et al.* (*7*) reported that the dissociation of CO occurs at 453 K on Ni(100) at pressures as low as 10^{-6} mbar. As the CO molecules with sufficiently high translational energy undergo dissociation in collisions on the terrace of the Ni surface (*13*), if CO molecules

FIG. 1. LEED pattern of carbided Ni(100) and Ni(111) surfaces at 72 eV. (a) (2 × 2)P4g pattern of carbided Ni(100). (b) Full-domain pattern of carbided Ni(111). (c) Single-domain pattern of carbided Ni(111).

are accommodated at the catalyst temperature, the CO molecules with high translational energy undergo dissociation on the surface. However, it is difficult to evaluate the relative contributions of the unimolecular dissociation and the dismutation reaction during catalysis. When hydrogen is removed from the gas phase, the amount of carbidic carbon intermediates on the surface will increase. In fact, when the Ni(100) or Ni(111) surface is exposed to CO at around 500 K, the deposition of carbidic carbon takes place rapidly not only on the surface but also in the subsurface. When this surface is heated in the UHV, the surface carbide decomposes at around 685 K (640 K in Ref. (*14*) is a systematic error) but one monolayer of graphite is built up concomitantly by the segregation of subsurface carbon. As a result, the LEED pattern changes from the carbide pattern to the graphite one at temperatures higher than 685 K. In contrast, when one monolayer of carbide, prepared by segregating carbon atoms from the bulk to surfaces, is heated in the UHV, the carbide layer decomposes at 685 K with no growth of graphite, so that a clean surface of p(1 × 1) is recovered (*14*). These results suggest that the epitaxial growth of graphite may require a supply of carbon atoms from the subsurface. The carbide segregated on Ni(100) and Ni(111) surfaces by annealing in the UHV for long periods is composed of one monolayer of carbide (*14*), which gives exactly the same LEED pattern as that obtained by the dismutation reaction of CO.

Figure 2 shows the hydrogenation of a p4g carbide layer prepared on the Ni(100) surface by the dismutation reaction of CO, where the (2 × 2)p4g carbide layer is about half of the full coverage of the p4g surface because of the half-maximal value of the $C_{KVV}/Ni_{LMM} = 0.4$. From the decay curve, the hydrogenation of the carbide layer is evaluated to be 4×10^{-4} sec^{-1} $site^{-1}$ at 450 K in 10 Torr of H_2, which is in surprisingly good agreement with the turnover frequency given by Goodman *et al.* (*1*) at 450–700 K for 120 Torr total pressure. This fact strongly suggests that the (2 × 2)p4g carbide overlayer corresponds to the intermediate in the methanation reaction. If this is the case, not only the p4g carbide on Ni(100) but also the carbide layer on Ni(111) surface would be reaction intermediates.

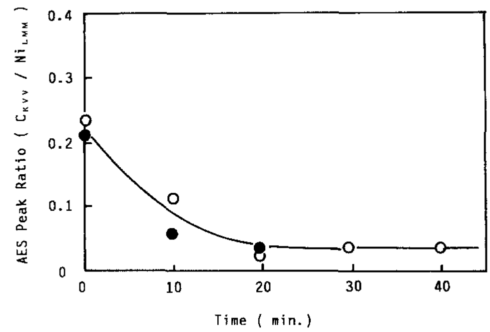

FIG. 2. Hydrogenation of p4g carbide overlayer on Ni(100) surface in 10 Torr of H_2 at 450 K. (●) Carbide was prepared at 450 K. (○) Carbide was prepared at 630 K.

Because the LEED pattern of the carbided Ni(111) surface is too complex for a direct resolution of the structure, McCarroll *et al.* (*15*) deduced a model by simulation. It was quite fortunate that we accidentally found the preferential growth of a single domain of the carbide layer on a Ni(111) surface during the segregration of carbon by annealing (*14*). Figure 1c shows the LEED pattern for a single domain carbide, which is expressed by

$$\begin{pmatrix} \frac{1}{2} + \sqrt{3}/\gamma, 1 \\ 1 - \sqrt{3}/\gamma, 2 \end{pmatrix}.$$

Based on this structure, the complex LEED pattern of the carbided Ni(111) surface can be reproduced as the three domains of carbide layer. It should be pointed out that this notation becomes exactly equal to the $(\sqrt{39} \times \sqrt{39})R16.1$ proposed by McCarroll *et al.* through the simulation method (*15*) when $\gamma = 5\sqrt{3}/9$.

Figure 3a shows a McCarroll model for the carbided Ni(111) surface, where the ratio of C to Ni atoms in a unit cell is $\frac{10}{45}$ =

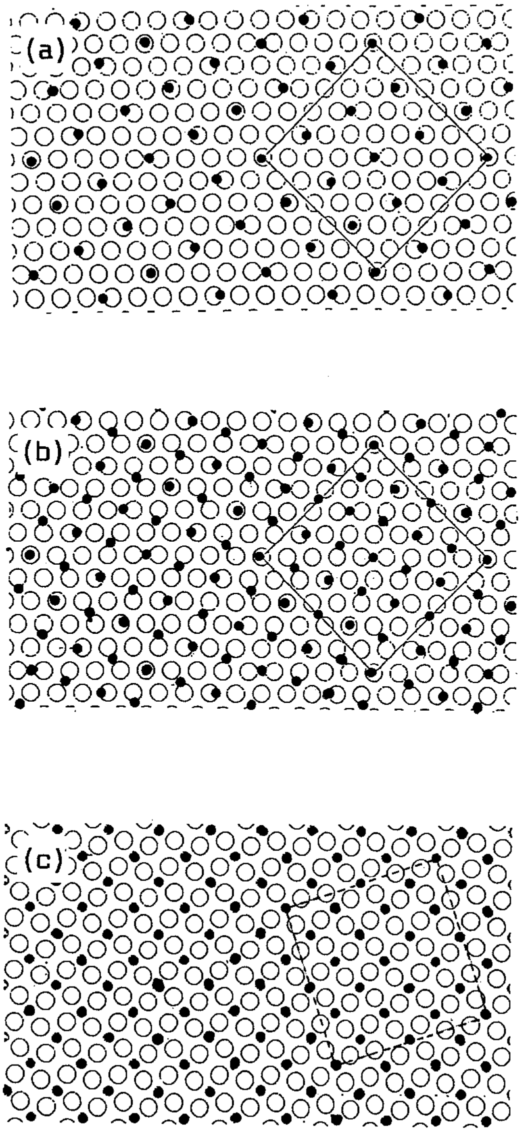

FIG. 3. Real space models for the carbide overlayer on Ni(100) and Ni(111) surfaces. (a) McCarroll model for carbided Ni(111), C/N = 10/45. (b) New model of carbide overlayer on Ni(111), C/Ni = 20/45. (c) (2 × 2)P4g model of carbide layer on Ni(100), C/Ni = 1/2.

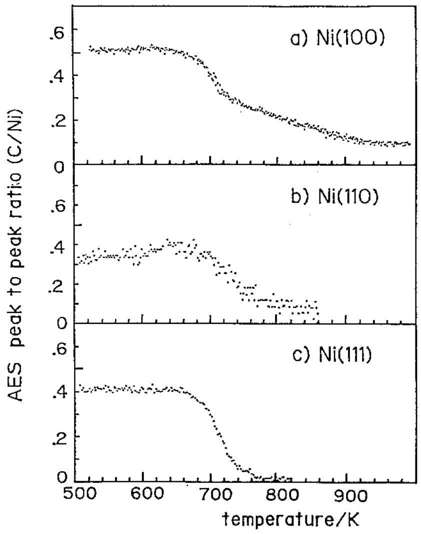

FIG. 4. Thermal decomposition of carbide overlayer formed on (a) Ni(100), (b) Ni(110), and (c) Ni(111) surfaces.

0.222. If this model is correct, the C/Ni ratio on the Ni(111) surface will be less than half that on the Ni(100) surface, because the C/Ni = $\frac{1}{2}$ for the (2 × 2)P4g structure on the Ni(100) surface (Fig. 3c). To confirm the ratio of C/Ni for the carbide on Ni(100) and Ni(111), one monolayer of carbide was carefully prepared on the Ni(111) as well as on the Ni(100) surface by segregating carbon atoms from the bulk at about 520 K. As shown in Fig. 4, the AES ratio of C_{KVV} to Ni_{LMM} on the Ni(111) surface is only slightly lower than that on the Ni(100) surface, which was confirmed by different runs. This fact indicates that the density of carbon atoms on the carbided Ni(111) is very similar to that of the p(2 × 2)P4g carbide on Ni(100) surface, and it is about double that of the McCarroll model. A new model of a double carbon density, C/Ni = 20/45 = 0.444, is proposed in Fig. 3b, where no reconstruction of Ni atoms is described.

If either Fig. 3b or 3c lies on the other model, the carbon atoms on the Ni(111) surface in Fig. 3b overlap completely with the p(2 × 2)P4g carbide on the Ni(100) surface in Fig. 3c.

The LEED pattern of the (2 × 2)P4g carbide on the Ni(100) surface has the characteristic missing spots (5), as shown in Fig. 1a, and it is noteworthy that similar missing spots can be recognized on the LEED pattern of a single-domain carbide grown on the Ni(111) surface shown in Fig. 1c. It should be pointed out that the McCarroll model shown in Fig. 3a will give no missing spots in the LEED pattern.

Taking these facts into account, we can conclude that the same carbide monolayer is grown on both Ni(111) and Ni(100) surfaces. This conclusion is supported by the same decomposition temperature of the carbide overlayer on the Ni(111), Ni(100), and Ni(110) surfaces; that is, the decomposition temperature of the carbide on Ni(111) and Ni(110) is very close to that of the p(2 × 2)P4g carbide on Ni(100) surface. As shown in Fig. 4, when the Ni(100), Ni(110), and Ni(111) surfaces covered with one monolayer of carbide are heated in the UHV, the surface carbon starts to decrease steeply at about 685 K on either surface of the Ni(100), Ni(110), or the Ni(111). That is, monolayer carbide undergoes decomposition at the same temperature, and the carbon atoms produced by the decomposition are rapidly diffused into the bulk instead of desorbing in the gas phase. Accordingly, we conclude that the methanation reaction on Ni(100), Ni(110), and Ni(111) surfaces is catalyzed by an identical compound to making carbide overlayer, and that this may be a reason why the methanation reaction proceeds at equal rates on Ni(100) and Ni(111) surfaces.

ACKNOWLEDGMENTS

This work was supported by a Grant-in-Aid for Scientific Research on Priority Areas (03205026) and a Grant-in-Aid (03640398) of the Ministry of Education, Science and Culture of Japan.

REFERENCES

1. Goodman, D. W., Kelley, R. D., Madey, T. E., and Yates, J. T., Jr., *J. Catal.* **63,** 226 (1980).
2. Goodman, D. W., *J. Vac. Sci. Technol.* **20,** 522 (1982).
3. Goodman, D. W., Kelley, R. D., Madey, T. E., and White, J. M., *J. Catal.* **64,** 479 (1980).
4. Wentrcek, P. R., Wood, B., and Wise, H., *J. Catal.* **43,** 363 (1976); Araki, M., and Ponec, V., *J. Catal.* **44,** 439 (1976); McCarty, J. G., and Wise, H., *J. Catal.* **57,** 406 (1979); Biloen, P., Helle, J. H., and Sachtler, W. H. M., *J. Catal.* **58,** 95 (1979); Tanaka, K., Yaegashi, I., and Aomura, K., *J. Chem. Soc. Chem. Commun.,* 938 (1982); Tanaka, K., Miyazaki, T., and Aomura, K., *J. Catal.* **81,** 328 (1983).
5. Dalmai-Imelik, G., and Bertolini, J. C., *Compt. Rend. (Paris) C* **270,** 1079 (1970). Onuferko, J. H., Woodruff, D. P., and Holland, B. W., *Surf. Sci.* **87,** 357 (1979).
6. Yamada, T., Misono, T., Tanaka, K., and Murata, Y., *J. Vac. Sci. Technol. A* **7,** 2808 (1989).
7. Astaldi, C., Santoni, A., Della Valle, F., and Rosei, R., *Surf. Sci.* **220,** 322 (1989).
8. Goodman, D. W., Kelley, R. D., Madey, T. E., and White, J. M., *J. Catal.* **63,** 226 (1980).
9. Sexton, B. A., and Somorjai, G. A., *J. Catal.* **46,** 167 (1977).
10. Krebs, H. J., and Bonzel, H. P., *Surf. Sci.* **88,** 269 (1979); **117,** 639 (1982).
11. Goodman, D. W., Yates, J. T., Jr., and Mady, T. E., *J. Catal.* **50,** 279 (1977).
12. Goodman, D. W., Yates, J. T., Jr., and Mady, T. E., *Surf. Sci.* **93** L135 (1980).
13. Tang, S. L., Lee, M. B., Yang, O. Y., Beckerle, J. D., Hines, M. A., and Ceyer, S. T., *J. Chem. Phys.* **82,** 2826 (1985). Lee, M. B., Beckerle, J. D., Tang, S. L., and Ceyer, S. T., *J. Chem. Phys.* **87,** 723 (1985).
14. Nakamura, J., Hirano, H., Xie, M., Matsuo, I., Yamada, T., and Tanaka, K., *Surf. Sci.* **222,** L809 (1989). Kasperkiewicz, J., and Palczewska, W., *Appl. Surf. Sci.* **17,** 477 (1984).
15. McCarroll, J. J., Edmonds, T., and Pitkethly, R. C., *Nature* **223,** 20 (1969).